DEVELOPMENT OF A COMBINED SPATIAL AND SPECTRAL METHOD FOR WEED DETECTION AND LOCALIZATION

J-B. VIOIX, J-P DOUZALS, J.W. LU
UMR CPAP Enesad Cemagref 21, Blvd Olivier de Serres 21800 QUETIGNY, FRANCE
Tel : 33 (0)3 80 77 27 48, fax : 33 (0)3 80 77 28 16, e-mail : jb.vioix@enesad.fr, jp.douzals@enesad.fr, jw.lu@enesad.fr
F. TRUCHETET
Le2i , IUT Le Creusot, 12, Rue de la Fonderie 71200 LE CREUSOT, FRANCE
Tel: 33 (0)3 85 73 10 92, fax : 33 (0)3 85 73 10 97, e-mail : f.Truchetet@iutlecreusot.u-bourgogne.fr
L. ASSEMAT
INRA, Unité de Malherbologie et Agronomie, BP 86510 21065 DIJON-CEDEX, France
Tel: 33 (0)3 80 69 32 85, fax : 33 (0)3 80 69 32 62, e-mail : assemat@epoisses.inra.fr

Abstract - **The aim of this study was to detect and localize weed patches in order to improve the knowledge on weed-crop competition. A remote control aircraft provided with a camera allowed to obtain low cost and repetitive information. Image processing was involved to detect weed patches. First the color information was used to separate the soil and plants through a shift of the colorimetric base. Then, a specific algorithm including Gabor filter detected crop row from the whole vegetation. The resulting image (crop image) was compared with the vegetation image and gave the main weed patches. Localization was realized with georeferenced landmarks also used for geometric correction. The last part of this paper deals with the development of a new acquisition device and its first results for the discrimination of weeds and crops using the spectral properties.**

1. INTRODUCTION

Weed detection was extensively studied as herbicide application has a relevant impact on economics and environment. Developing a spraying strategy in the context of precision agriculture needs to improve in-field detection of weeds.
Weed detection was directed through different approaches. First experimental works were based on the spectral signature of weeds and crops. Vrindts et al. [6] determined some specific spectral bands to achieve weed identification. Statistical analysis were conducted to find spectral properties of each species. In the same way Pollet et al. [3] developed an imaging spectrograph. This device gave an image with the spatial dimension on vertical axis and the spectral dimension on horizontal axis. Another experimental method was based on morphological properties extracted from leaf shape [2]. In this case high resolution images was needed. Moreover computation time were very important and limited this application to small areas.
In-field detection of weeds was also possible on stubble. Biller et al. [1] achieved a sensor to detect plants on bare soil. Two optical bands as red (650 nm) and infra-red (850 nm) were used to find green plants. The difference between the two wavelengths was determined and controlled online spraying. Finally last method concerned remote sensing imaging. For example aerial images taken with four camera equipped with optical band-pass filters were used by Rew et al. [4] to find wild oat in triticale crop through the normalized difference vegetation index (NDVI). They shown the increase in NDVI with wild oat infestation.
All these previous approaches were conducted in order to discriminate weeds and crops from their spectral signature or shape. The objective of this research program is to develop combined spectral and spatial methods upon aerial photographs in order to improve weed detection and localization.

2. ACQUISITION AND PREPROCESSING

A. Image acquisition

A remote control aircraft was customized for this application. A camera Olympus µII (aperture of 1:2.8 and focal of 35 mm) was placed in the hold; the shot was trigged by the remote control. A miniature video camera and an embedded high frequency (HF) emitter gave online images of the flying over area on a TV. As the resolution depended only on the fly altitude, the drone was able to fly from an about ten meters up to few hundred meters. The resulting resolution was found to vary from less than a centimeter per pixel up to some meters per pixel. After developing, films were digitalized using a Canon CanoScan D660U scanner. 1702 by 1136 pixels images on red, green, blue (R,G,B) channels were obtained. Theses images were then saved in BMP format to avoid compression loses.

B. Georectification

To keep a good resolution, we only used low altitudes images, so several shots were needed to get the whole field. Landmarks were placed and georeferenced in the field using D-GPS coordinates to locate images and also to give black and white levels. A specific algorithm gave the transformation matrix between image coordinates and GPS coordinates.

3. IMAGE PROCESSING

A. Ground and plants discrimination

Two methods are generally employed upon color images to solve this problem: texture analysis or color discrimination. In most cases the first method is very efficient but accuracy depends on soil roughness (due to clods, implements prints…) and needs high cost time algorithms. The second method is based on the color properties between soil and vegetation.
In this case the R,G,B color base is not adapted to find accurate colorimetric information on images acquired under natural light. Indeed, color levels depend on lightness, that has to be separated from chromatic values. The HSV (hue, saturation, value) color base allows this separation but RGB-HSV transformation appears to be non linear and unstable for low RGB values. Steward and Tian ([5]) described another color base (which is linear) more adapted to vegetation images.

$$\begin{bmatrix} V_1 \\ V_2 \\ I \end{bmatrix} = \begin{vmatrix} -\frac{1}{\sqrt{2}} & \frac{1}{\sqrt{2}} & 0 \\ -\frac{1}{\sqrt{6}} & \frac{1}{\sqrt{6}} & \frac{2}{\sqrt{6}} \\ \frac{1}{\sqrt{3}} & \frac{1}{\sqrt{3}} & \frac{1}{\sqrt{3}} \end{vmatrix} \cdot \begin{bmatrix} R \\ G \\ B \end{bmatrix} \quad (1)$$

This equation (1) describes a base rotation. The three vectors are unitary and perpendicular, so the information are fully independent. I corresponds to the luminosity vector, so shadows and other lightness defaults are only on this one.
(V_1, V_2) provide a colorimetric plane. V_1 is defined as the difference between red and green channels. So for vegetation V_1 is positive and is negative for ground. For the next processing, only positive values of V_1 are kept.

B. Seed frequency characterization

Previous image treatments led to vegetation images including crops and weeds. With the assumption that crops corresponded to repetitive structures, the Fourier's transform operation (by a frequency domain conversion) was tested. In this case each pixel was individually analyzed through his spatial distribution and V1 intensity. The Fourier's transform result corresponded to the period and the rotation angle of periodic structures. For further task, the seed frequency have to be characterized. A sweeping line is used to find the angle of the seed frequency with the horizontal axis. Let φ this angle, the equation of a segment starting at the origin can be written as :

$$\begin{cases} x = t\cos\varphi \\ y = t\sin\varphi \end{cases} \quad (2)$$

The sum of the TF along this line is the integral of the TF for this angle.

$$S(\varphi) = \sum_{t}^{x \le X \text{ and } y \le Y} TF(x, y) \quad (3)$$

with X and Y the limits of the TF.

We increase φ from 0 to π. $S(\varphi)$ is normalized by the length of the line, give by the last value of t. The figure 1 show the evolution of $S(\varphi)$. The maximum value of $S(\varphi)$ gives the angle of the frequency..
Then, the seed frequency is find using the TF for this angle. The figure 2 shows the TF for the maximum angle.

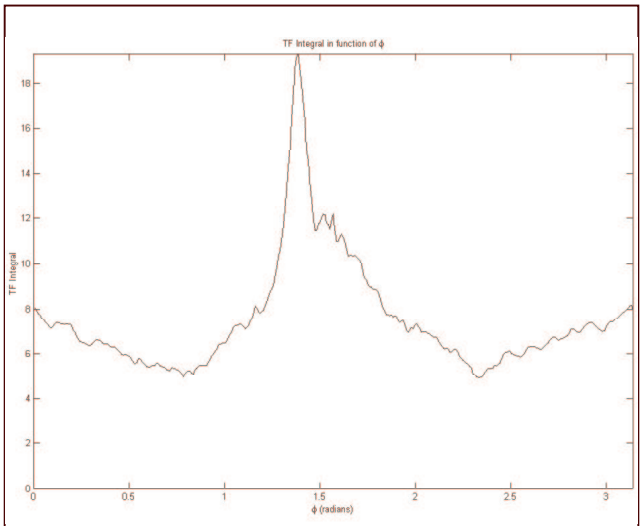

Fig. 1 : Value of $S(\varphi)$ from 0 to π

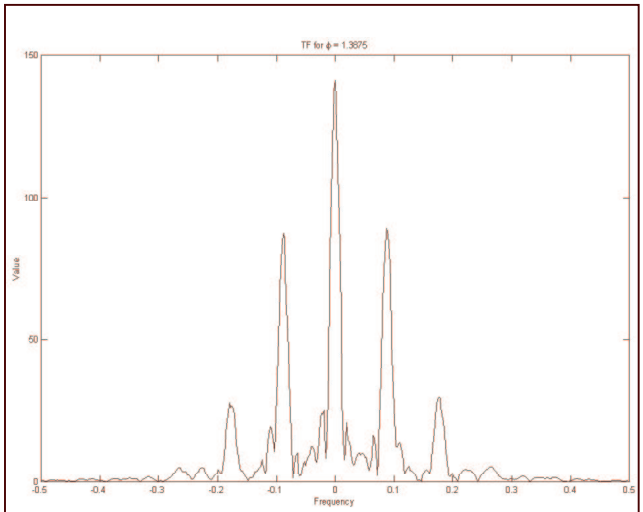

Fig. 2 : TF for φ=1.3875

C. Low frequencies enhancement

These last information allowed for example the filtering of the image by adjustment of the rotation angle and frequency. First trials showed that the seed frequency had often a very low value generally making the filtering difficult. The size of the filter kernel depends on the frequency, a low frequency involves a big kernel, with inaccurate results and very long computation time. To minimize this constrain a dilation of the lowest must be achieved. The easiest way is an under-sampling of the image by removing a line and a column on two. This step is recursively repeat to obtain a frequency which allows an accurate filtering.

D. Gabor filter

The filter is a band pass directive filter along the R_1 axis. It was centered on ω, σ_x and σ_y set the band width respectively along the R_1 axis and the R_2 axis. Periodic structures with a frequency near ω and a rotation angle close to φ value were unchanged other were deeply faded.

$$g(x,y) = \frac{2}{\pi\sigma_x\sigma_y}\exp\left(-\frac{R_1^2}{\sigma_x^2}-\frac{R_2^2}{\sigma_y^2}\right)\cos(2\pi\omega R_1) \qquad (4)$$

$$\text{with } \begin{cases} R_1 = x\cos\varphi + y\sin\varphi \\ R_2 = -x\sin\varphi + y\cos\varphi \end{cases}$$

The spatial representation of $g(x,y)$ is shown in figure 1, the FFT in figure 2. It is a directive band pass filter centered on ω, and oriented by φ. The width is defined by σ_x and σ_y. After sampling, a mask can be defined. The size of the mask is depending on σ_x and σ_y. We truncate $g(x,y)$ on the interval $[-3\sigma, 3\sigma]$, where σ is the maximum of (σ_x, σ_y). We keep a good approximation with a acceptable filter size.

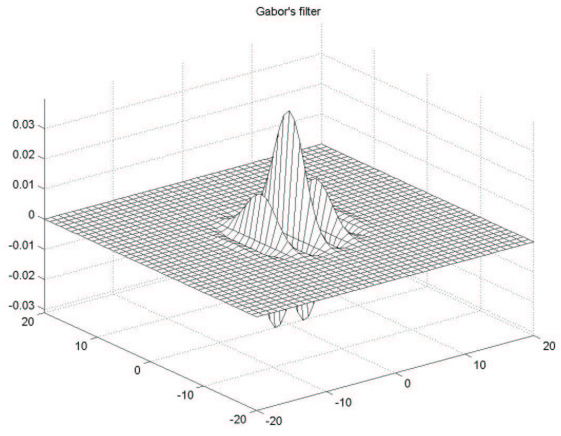

Fig. 3 : Gabor filter

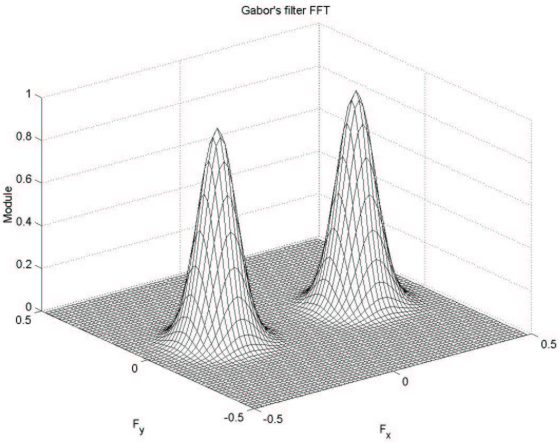

Fig. 4 : Fast Fourrier Transform of Gabor filter

E. Gain computing

After filtering, the crops would have low value. A thresholding can be considered, but the results are not satisfying. On V_1 vector, crops and weeds have spread values. So after filtering a low value obtained can be due to a weed pixel with high V_1 value, or a crop pixel with a low V_1 value. Then we decided to compute the gain of each pixel for an accurate thresholding. For each point (x,y) which its value on V_1 is strictly positive, the gain is computed as:

$$G(x,y) = \frac{p_g(x,y)}{p_{v_1}(x,y)} \qquad (5)$$

In this equation (5), $p_g(x,y)$ is the module of the point after filtering, and $p_{v_1}(x,y)$ the value of this point on the vector V_1. If the gain is near 1, the point belongs to a periodic structure defined by the coefficients of the Gabor filter. For thresholding, a level of –3 dB (0.707) is generally chosen. A lowest value increases the band width, a higher one diminishes it. Before this operation, the image is resized to its original size due to the previous under-sampling.

F. Results

This approach is similar to wavelets. In a wavelets analysis, all frequencies are proceeded. In our analysis, only the interesting ones are chosen, with a consequent reduction of computing time and memory size.
We first decided to test this algorithm on synthesis images to confirm the validity of the method. After this step, we tried it on various crops. Results depended on species and vegetation stages.
Crops with an important spreading out as rape and barley

gave bad results. Indeed the space between two rows was rapidly hidden by foliage during the vegetation growth. So the discrimination was impossible with only this method. The FFT did not give the seedling frequency, so the Gabor filter can not be tuned.
On other species the identification gave better results, and the weeds can be found at early stage. The figure 5 shows an image of a corn field (6 per 3 meters with a resolution of around 5 mm per pixel). Some weeds can be noticed between two rows. The figure 6 shows the V_1 vector (in inverted video). After the treatment, the crops are hidden in black, and only the weeds appear as vegetation (figure 7). The end of some crop foils are detected as weeds, it is due the foil shape which is too elongated, and the diminution of the resolution during the enhancement of the lowest frequencies.

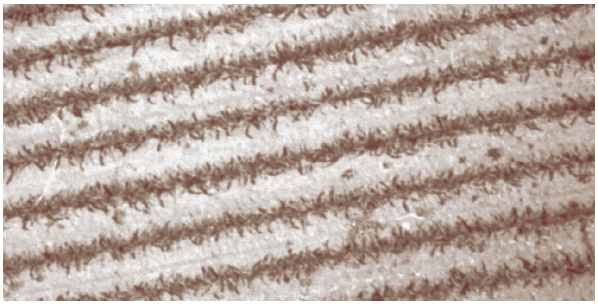

Fig. 5 : Source image (corn field)

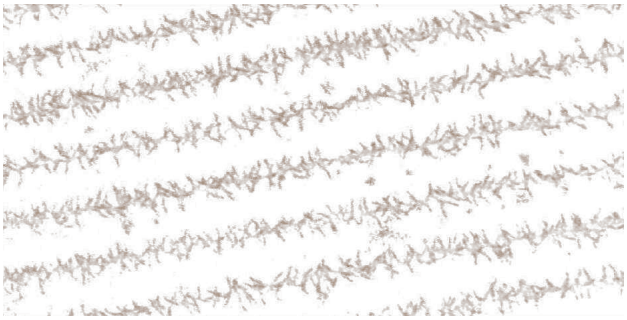

Fig. 6 : V1 image (inverted video)

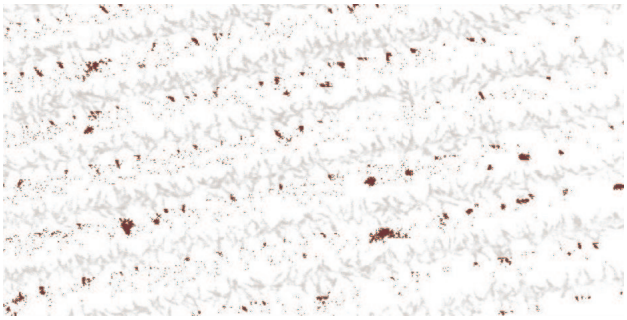

Fig. 7 :Result image (weeds in black, other vegetation in gray)

4. FIRST WORKS ON SPECTRAL PROPERTIES

A. Development of a new acquisition device

As explain in the first part, the infra-red gives some interesting information for this application. So, with the three visible band (red, green, blue), images will be composed of four band. We work on a new acquisition device equipped with a CCD sensor and a disc with four filter. This disc rotates in front of the sensor. The exposure time can set at different values depending on the filter bandwidth.
The first tries of this system were done with some onion crops with weeds. A set of four filter was used. Two filters are band pass, one in blue (bandwidth : 50 nm, central wavelength : 500 nm) and the other in the green (bandwidth : 75 nm, central wavelength : 550 nm). The two others filters are high-pass at 675 nm (red) and 750 nm (infra-red).

B. Crops and weeds separation using the PCA

With multicomponent images, statistical tools can be applied. The principal component analysis (PCA) is often used to find the base which gives the best decorrelation. In our case, we can consider each pixel as a vector of 4 components : $p_{i,j} = \begin{pmatrix} V_1 \\ V_2 \\ V_3 \\ V_4 \end{pmatrix}$ with i, j the coordinates of the pixel and $V_1 \ldots V_4$ the values of this pixel on the four wavelengths. We can define the covariance matrix of this image as :

$$C = \frac{1}{N} \sum_{i,j} (P_{i,j} - \overline{P}).(P_{i,j} - \overline{P})_T \qquad (6)$$

where N is the number of pixel in the image and $\overline{P}$ the mean vector of $P_{i,j}$. The eigenvectors of the matrix C give the base where the decorrelation is maximum.
The principal component analysis was been tried to find some difference between crops and weeds. It was computed only on the plant pixel to improve the discrimination. Some little variation were find on the less significant vector. But, a simple threshold can not be found this difference.
The major limitation of the PCA is due to its linearity. The PCA gives the linear combination of the input vectors. If the vector are correlated with a non-linear combination, the PCA gives bad results.

C. Crops and weeds separation using a neural network

Considering the variability between two images, a learning classifier can be an interesting solution [9]. In this case, few pixels are classified by the operator and the system learns the principal characteristics of this train set. For the

first tries, a very simple network was been developed. The input vector is the value of the pixel on the four wavelengths. The input layer was composed of 8 cells with a linear activation function. The internal layer had the same number of neurons but with a sigmoid function. Then, the output layer was composed of 2 neurons (W and C) with also a sigmoid function. The following learning rules were used.

	Neuron W	Neuron C
Crop	0.1	0.9
Weed	0.9	0.1
Soil	0.1	0.1

The value of 0.1 and 0.9 are prefer than respectively 0 and 1 for a better learn. Two training sets were tested. They both have ten pixels of crops and ten pixels of weeds, but one include ten pixels of soil, not the other. Only the pixels of vegetation were computed with the network.
The result were slightly better with the including of some soil pixel. The edge pixels were bad classified when the soil is not used in the training set. The figure 8 shows the infra-red band of the source image. The figure 9 and 10 show the result of the two neurons. A simple threshold (equal to 0.5) was applied to obtain theses images. Considering the quality of the images, the results are interesting. For example, on the top right corner a field bindweed[0] leaf is cover by an onion leaf. After classification, the both plants are well classified. The edge are noisy, a region growth algorithm can be applied to reduce this problem.

5. CONCLUSION AND ENHANCEMENT

The combination of this two method must be studied. Merging tools as fuzzy logic can be used to done this task. Some other information must be add as texture, shape, …
The multispectral sensor is still under development. Some improvement are in project. It must be able to store images on-line for an embedded use. At the present time, the exposure time can be accurate tuned.
The choice of filter wavelengths can be improve to give more information. Theses filters will be chosen accordingly with the crops species.

6. ACKNOWLEDGEMENT

This project is financed by ITCF (French Institute of Cereal and Forage) and the council of Burgundy.

7. REFERENCES

[1] Biller R.H., Hollstein A., Sommer C. (1997). Precision Application of Herbicides by Use of Optoelectronic Sensor. Precision Agriculture 1997, BIOS Scientific Publishers Ltd, 451-458.

[2] Manh A.-G., Rabatel G. Assemat L. (2000) Caractérisation morphologique de population d'aventices par vision numérique de terrain, Agriculture de précision – Avancées de la recherche technologique et industrielle, Educagri éditions, 183-195

[3] Pollet P. Feyaerts F., Wambacq P., Van Gool L. (1998) Weed Detection Based on Structural Information Using an Imaging Spectroghraph, Proceedings of the Fourth International Conference on Precision Agriculture, ASA-CSSA-SSSA, 677 South edge Road, Madisson, WI 53711, 1579-1591

[4] Rew L.J., Lamb D.W., Weedon M.M., Lucas J.L., Medd R.W., Lemerle D. (1999) Evaluating Airborne Multispectral Imagery For Detecting Wild Oats in a Seedling Triticale Crop, Precision Agriculture '99, J.V. Stafford, Sheffield Academic Press, 265-274

[5] Steward B. L., Tian L. F. (1999) Machine-vision Weed Density Estimation for Real-time, Outdoor Lighting Conditions, Transactions of the ASAE, Vol. 42(6), 1897-1909

[6] Vrindts E., de Baerdemaeker J. (1997) Optical Discrimination of Crop ,Weed and Soil for On-line Weed Detection, Precision Agriculture 1997, BIOS Scientific Publishers Ltd, 537-544

[7] Yonekawa S., Sakai N., Kitani O. (1996) Identification of Idealized Leaf Types Using Simple Dimensionless Shape Factors by Image Analysis, Transactions of the ASAE, Vol. 39(4), 1525-1533

[8] Guyer D. E., Miles G. E., Gaultney L. D., Schreiber, M. M. (1993) Application of Machine Vision to Shape Analysis in Leaf and Plant Identification, Transactions of the ASAE, Vol. 39(4), 1525-1533

[9] Moshou D., Ramon H., de Baerdemaeker J., (1999) Neural Network Based Classification of Different Weed Species and Crops, Precision Agriculture '99, J.V. Stafford, Sheffield Academic Press, 275-284

[0] *Con□ol□us ar□ensis* □

Fig. 8 : Image source (infra-red band)

Fig. 9 : Image result of the neuron W after thresholding.

Fig. 10 : Image result of the neuron C after thresholding.